Chinese Chemical Letters 33 (2022) 3151–3155

Contents lists available at ScienceDirect

Chinese Chemical Letters

journal homepage: www.elsevier.com/locate/cclet

Colorimetric and electrochemical detection of ligase through ligation reaction-induced streptavidin assembly

Yaliang Huang[a,b], Ting Sun[b], Wendi Li[c], Lin Liu[b,*], Gang Liu[b], Xinyao Yi[a], Jianxiu Wang[a,*]

[a] Hunan Provincial Key Laboratory of Micro & Nano Materials Interface Science, College of Chemistry and Chemical Engineering, Central South University, Changsha 410083, China
[b] Henan Province of Key Laboratory of New Optoelectronic Functional Materials, Anyang Normal University, Anyang 455000, China
[c] Sanquan College of Xinxiang Medical University, Xinxiang 453003, China

ARTICLE INFO

Article history:
Received 29 July 2021
Revised 5 October 2021
Accepted 14 October 2021
Available online 22 October 2021

Keywords:
Ligase
Electrochemical analysis
Streptavidin
Gold nanoparticles
Colorimetric assay
Electrochemical impedance spectroscopy

ABSTRACT

We propose a concept for ligase detection by conversion of aggregation-based homogeneous analysis into surface-tethered electrochemical assay through streptavidin (SA)-biotin interaction. Sortase A (SrtA) served as the model analyte and two biotinylated peptides (bio-LPETGG and GGGK-bio) were used as the substrates. SrtA-catalyzed ligation of the peptide substrates led to the generation of bio-LPETGGGK-bio. The ligation product (bio-LPETGGGK-bio) induced the aggregation and color change of SA-modified gold nanoparticles (AuNPs) through the SA-biotin interactions, which could be assayed by the colorimetric method. Furthermore, we found that the bio-LPETGGGK-bio could trigger the assembly of tetrameric SA proteins with the formation of the $(SA\text{-bio-LPETGGGK-bio})_n$ assemblies through the same interactions. The above results were further confirmed by atomic force microscopy and fluorescent imaging. The insulated assemblies were *in-situ* fabricated at the SA-modified gold electrode, thus hindering the electron transfer of $[Fe(CN)_6]^{3-/4-}$ and leading to an increase in the electron-transfer resistance. The capability of the method for the detection of SrtA both *in vitro* and *Staphylococcus aureus* (*S. aureus*) has been demonstrated. SrtA with a concentration down to 1 pmol/L has been determined by the electrochemical analysis, which is lower than that achieved by the colorimetric assay (50 pmol/L). By integrating the advantages of homogeneous reaction and heterogeneous detection, the strategy serves as an ideal means for the fabrication of various sensing platforms by adopting biotin-labeled and sequence-specific peptide or nucleic acid substrates.

Protein/peptide modification is of great significance and particular interest in the field of biological science and protein therapeutics. Peptide ligases are a kind of enzymes that can catalyze the formation of peptide bonds with high site and substrate selectivity, including sortase, butelase, trypsiligase, subtiligase, peptiligase and omniligase [1,2]. The enzymes play a vital role in protein engineering, chemical labeling and peptide/protein macrocyclization [3–5]. In addition, changes in the enzymatic activity and level of ligases have been closely related to many diseases, such as skin and soft tissue infections, osteomyelitis, meningitis, endocarditis, septicemia, and toxic shock syndrome [6,7]. Consequently, ligases serve as potential biomarkers and therapeutic targets. Accurate and sensitive detection of ligases is of great significance in biological research, medical diagnostics and pharmaceutical development. The common methods for quantitative detection of ligases include high-performance liquid chromatography and mass spectrometry [8,9]. These homogeneous methods can directly monitor the catalytic product, but usually suffers from complex processes, poor sensitivity and complicated instrumentation. Alternatively, ligases have been determined by using fluorophore- and quencher-labeled substrates based on fluorescence quenching or fluorescence resonance energy transfer [10–13]. The fluorescent methods are sensitive and effective but possess certain drawbacks, such as low signal-to-background ratio, high cost as well as complex procedures for the substrate synthesis. Therefore, it is still desirable to develop simple, sensitive and cost-effective methods for detection of ligases and screening of their potent inhibitors.

In recent decades, gold nanoparticles (AuNPs)-based colorimetric methods have been used for bioassays due to the advantages of easy operation, fast response, good sensitivity and simple instrumentation. Biotin-functionalized peptides and those containing cysteine and/or positively charged amino acids can induce the

* Corresponding authors.
E-mail addresses: liulin@aynu.edu.cn (L. Liu), jxiuwang@csu.edu.cn (J. Wang).

https://doi.org/10.1016/j.cclet.2021.10.038
1001-8417/

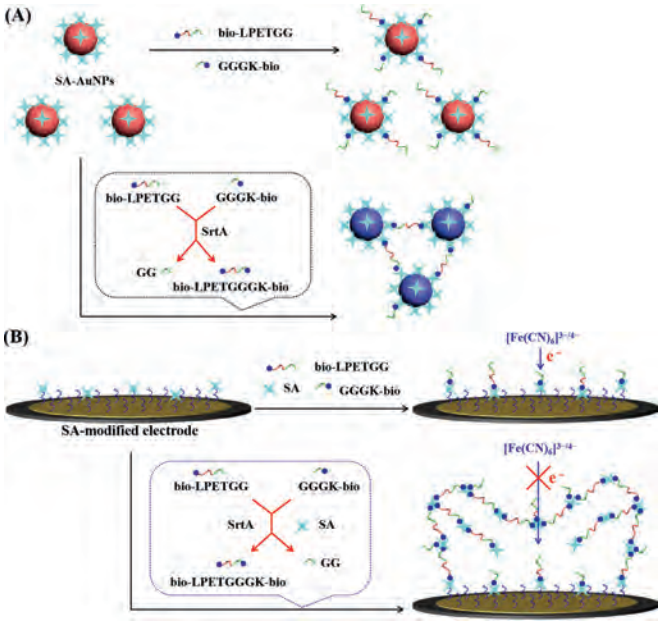

Scheme. 1. Schematic representation of colorimetric (A) and electrochemical (B) assays of SrtA by ligation product-induced aggregation of SA-AuNPs or SA through the SA-biotin interactions.

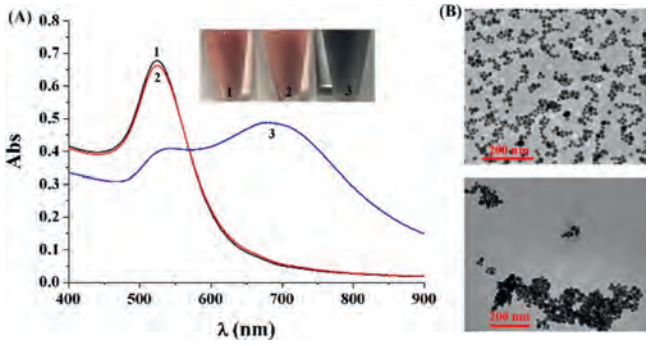

Fig. 1. (A) UV–vis absorption spectra and photographic images of SA-AuNPs in the absence (tube/curve 1) and presence of 1 μmol/L of bio-LPETGG and GGGK-bio (tube/curve 2) or 0.5 μmol/L bio-LPETGGGK-bio (tube/curve 3). (B) TEM images of SA-AuNPs in the absence (top) and presence (bottom) of bio-LPETGGGK-bio.

aggregation of AuNPs through the streptavidin (SA)-biotin, Au-S or electrostatic interactions [14–17]. This phenomenon has allowed for the colorimetric detection of proteases by cleaving the peptide into two shorter parts, which limits the substrate-induced AuNPs assembly. In this work, we found that the two biotinylated peptides can be conjugated by a ligase and the resulting ligation product can induce the aggregation of SA-modified AuNPs through the SA-biotin interactions (Scheme 1A). Thus, a colorimetric method for the detection of peptide ligases was proposed using SA-AuNPs as the color indicators. Though simple and convenient for ligase inhibitor screening, the colorimetric assay exhibits low sensitivity for ligase detection in biological samples. Electrochemical methods are sensitive to the peptide cleavage event occurring on the liquid-solid interface, thus allowing for the detection of proteases with high sensitivity. Recent investigations indicate that the metal ions- and peptides-induced aggregation of AuNPs or AgNPs can be initiated on the electrode, thus infusing the aggregation events into the interface [18–21]. SA is a tetrameric protein with four biotin-binding sites, and the SA-biotin system has been widely used to develop various biosensors [22–24]. We found that the ligation product with two biotin tags could induce the assembly of not only SA-AuNPs but also SA proteins through the SA-biotin interactions. Thus, we proposed that the liquid-phase assay of ligase can be transformed into electrochemical analysis through the product-triggered formation of SA-biotin-peptide networks on the SA-covered electrode (Scheme 1B). The resulting networks can efficiently limit the electron transfer of $[Fe(CN)_6]^{3-/4-}$ through the formation of insulating protein/peptide layers, and the change of electron transfer resistance can be conveniently monitored by electrochemical impedance spectroscopy (EIS). The conventional peptide-based electrochemical methods involve the immobilization of peptides on the electrode surface, which limits the interaction between the enzyme active center and the reaction site of peptide due to the steric hindrance effect [25–27].

Sortase A (SrtA) is a kind of thiol-containing transpeptidase prevalent in Gram-positive bacterias [28]. The ligase can recognize the substrate bearing a "sorting sequence" of LPXTG and cleave the peptide bond between threonine and glycine [29,30]. The N-terminal glycine of another protein/protein can attack the acyl-enzyme intermediate to yield a new peptide bond. The feasibility of our method for the assay of SrtA has been tested. Two biotinylated peptides with the sequences of bio-LPETGG and GGGK-bio were rationally designed as the substrates [31]. SrtA-catalyzed transpeptidation allowed the ligation of the peptide substrates with the formation of bio-LPETGGGK-bio. Since peptides and nucleic acids can be easily labeled with biotin groups in solid phase synthesis, the sensing protocol can be extended for the construction of versatile platforms for determining other ligases and screening potent inhibitors.

The aggregation of AuNPs can lead to a distinct red shift of the localized surface plasmon resonance (LSPR) band. Based on the SA-biotin interactions, various AuNPs-based colorimetric biosensors have been designed by using biotinylated peptides or nucleic acids as the probes [17,20,32-35]. By examining the changes in the color and LSPR band of SA-AuNPs, colorimetric assay of SrtA was conducted. Modification of SA on the surface of AuNPs did not induce significant change in the LSPR band of AuNPs (Fig. S1 in Supporting information). We also found that the modification improved the stability of AuNPs to resist the salt-induced aggregation, which is in agreement with the previous reports [34,35]. No significant changes in the color and LSPR band of AuNPs at 525 nm were observed with the addition of two substrate peptides bio-LPETGG and GGGK-bio (cf. tube/curve 1 and tube/curve 2 in Fig. 1A). This indicates that the SA-AuNPs are stable in the presence of the substrate peptides. However, incorporation of bio-LPETGGGK-bio caused the color change from red to blue (tube 3), which is accompanied by the LSPR band shift from 525 nm to 670 nm (curve 3). The LSPR band change was linearly dependent upon the bio-LPETGGGK-bio concentration in the range of 1–500 nmol/L. These results indicated the capability of bio-LPETGGGK-bio to induce the aggregation of SA-AuNPs, which was further confirmed by the TEM observation (Fig. 1B).

When the substrate peptides (bio-LPETGG and GGGK-bio) were incubated with SrtA, the color of SA-AuNPs suspension became blue and a red shift of the LSPR band was observed (Fig. S2A in Supporting information). The sensing protocol thus provides a viable means for the assay of SrtA. It was found that the color change and band shift were dependent upon the SrtA concentration, and the level of bio-LPETGGGK-bio increased and that of peptide substrates decreased accordingly with the proceeding of SrtA-catalytic ligation. The relative absorption intensity, defined as A_{670}/A_{525}, was used to evaluate the analytical performances, where A_{670} and A_{525} were referred to the absorption intensities at 670 and 525 nm, respectively. The A_{670}/A_{525} values were intensified while increasing the concentrations of SrtA in the range of 0–2 nmol/L (Fig. S2B in Supporting information). Sortase serves as a potential target for the development of effective antiviral drugs,

while berberine chloride, a natural plant alkaloid found in many Chinese herbs, can inhibit the activity of SrtA [11]. Based on the colorimetric assay, berberine chloride was found to inhibit SrtA activity in a dose-dependent manner. The half-maximal inhibitory concentration (IC_{50}) in the case of 2 nmol/L SrtA was found to be 0.76 μg/mL, being consistent with that obtained by the fluorescent assay [11].

Although the AuNPs-based colorimetric method is simple, easy to operate, and does not require any special equipment, it possesses a lower sensitivity for SrtA detection than the reported fluorescent methods [11,13]. EIS is a simple and sensitive method for measuring the immobilization and binding processes occurring at the electrode surface. Inspired by the binding of one tetrameric SA toward four biotin molecules and biotinylated peptide-induced aggregation of SA-AuNPs through SA-biotin interactions, we envisioned that the tetrameric SA could be assembled on the SA-modified electrode with bio-LPETGGGK-bio as the linker, thus infusing the colorimetric principle into the electrochemical assay. The schematic for SrtA detection is depicted in Scheme 1B. In the absence of SrtA, the substrate peptides of bio-LPETGG and GGGK-bio could bind to the SA proteins anchored on the electrode and existing in solution, thereby inhibiting the further assembly process. After ligation of the peptide substrates by SrtA, the catalytic product of bio-LPETGGGK-bio was captured by the SA-modified electrode. The biotin group at the other end of the captured peptide allowed the attachment of SA protein in solution. Through the SA-biotin interactions, more and more catalytic products and SA proteins in solution could be continually recruited to the electrode surface. The resulting $(SA\text{-}bio\text{-}LPETGGGK\text{-}bio)_n$ assemblies thus hindered the electron transfer and significantly increased the impedance response due to their large size and negative charges.

Atomic force microscopy (AFM) can provide information concerning the surface morphology and structure of the nanomaterials. To prove that the peptide of bio-LPETGGGK-bio can induce the SA assembly, the morphologies of SA and SA/bio-LPETGGGK-bio were characterized by AFM. As shown in Fig. 2A, the SA proteins coated on the mica surface were dispersed uniformly. Recall that the 66-kDa SA is a globular tetrameric protein with a diameter of 1–2 nm [17]. Incubation of SA with bio-LPETGGGK-bio resulted in the formation of the aggregates of $(SA\text{-}bio\text{-}LPETGGGK\text{-}bio)_n$ assemblies. In contrast, no particles or aggregates were formed on the mica surface treated with bio-LPETGGGK-bio.

The feasibility of the method for EIS assay of SrtA was demonstrated by incubating the SA-modified electrodes with different sample solutions. As shown in Fig. 2B, there is no significant change in the electron-transfer resistance (R_{et}) when the SA-modified electrode (curve a) was incubated with the SrtA reaction buffer (curve b), the mixture of bio-LPETGG, GGGK-bio and SA (curve c) or the catalytic product of bio-LPETGGGK-bio (curve d). However, a remarkably increased R_{et} was observed upon incubation of the SA-modified electrode with bio-LPETGGGK-bio/SA mixture (curve e), indicating the formation of insulating $(SA\text{-}bio\text{-}LPETGGGK\text{-}bio)_n$ assemblies. The *in-situ* formed assemblies could effectively block the electron transfer of $[Fe(CN)_6]^{3-/4-}$ and the R_{et} increased with the bio-LPETGGGK-bio concentrations in the range of 0.01–1 μmol/L. When the SA-modified electrode was incubated with the mixture of bio-LPETGG, GGGK-bio, SrtA and SA (curve f), the impedance was also greatly enhanced. The enhanced R_{et} suggested the capability of SrtA for catalyzing the transpeptidation reaction, which thus resulted in the generation of bio-LPETGGGK-bio and then the $(SA\text{-}bio\text{-}LPETGGGK\text{-}bio)_n$ assemblies. Conversely, smaller R_{et} was attained when the SA-modified electrode was treated with the bio-LPETGG/GGGK-bio/SA mixture (curve c) or the bio-LPETGG/GGGK-bio/SrtA mixture (curve g). The EIS results were also confirmed by fluorescence microscopy using FITC-SA instead

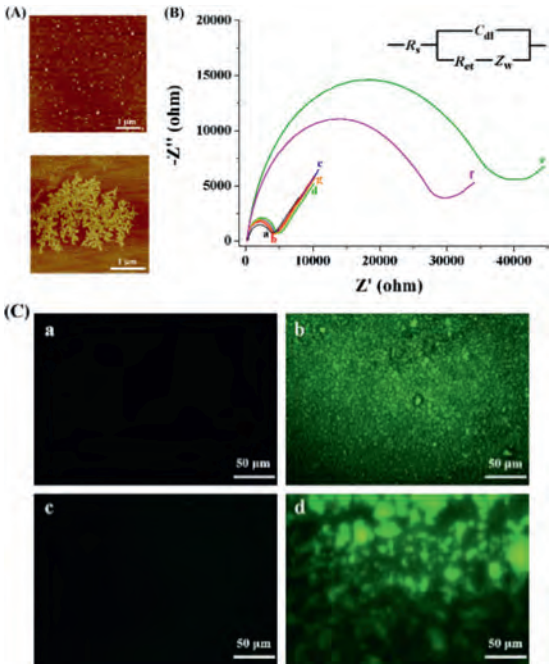

Fig. 2. (A) AFM images of 0.5 μmol/L SA before (top) and after (bottom) interaction with 0.5 μmol/L bio-LPETGGGK-bio. (B) EIS responses at the SA-modified electrode before (curve a) and after incubation with the following solutions: SrtA reaction buffer (b), bio-LPETGG + GGGK-bio + SA (c), bio-LPETGGGK-bio (d), bio-LPETGGGK-bio + SA (e), bio-LPETGG + GGGK-bio + SrtA + SA (f), and bio-LPETGG + GGGK-bio + SrtA (g). The concentrations of bio-LPETGG, GGGK-bio, bio-LPETGGGK-bio, SA and SrtA used were 2 μmol/L, 2 μmol/L, 1 μmol/L, 0.5 μmol/L and 0.2 nmol/L, respectively. (C) Confocal fluorescent images of SA-modified gold chips before (a) and after incubation with bio-LPETGGGK-bio/FITC-SA (b), bio-LPETGG/GGGK-bio/FITC-SA (c) or bio-LPETGG/GGGK-bio/SrtA/FITC-SA (d).

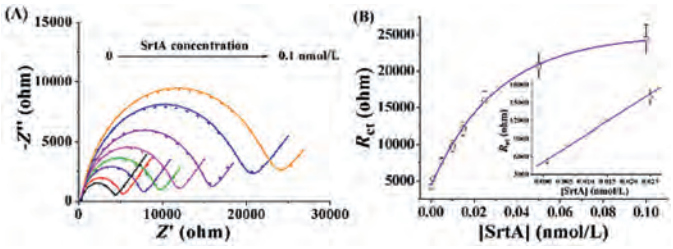

Fig. 3. (A) EIS responses at the SA-modified electrode in the case of SrtA with various concentrations (0, 0.001, 0.005, 0.01, 0.015, 0.025, 0.5 and 0.1 nmol/L). The experimental data and fitted results were shown as the points and curves, respectively. (B) Dependence of R_{et} on SrtA concentration. The inset depicts the linear portion of the curve.

of SA. As shown in Fig. 2C, the SA-modified chip surface was black (panel a), and green assemblies were observed on the chip after incubation with bio-LPETGGGK-bio/FITC-SA mixture (panel b), evidencing bio-LPETGGGK-bio-induced *in-situ* assembly of FITC-SA. Interestingly, no or fewer green assemblies were attained on the bio-LPETGG/GGGK-bio/FITC-SA-treated chip (panel c), but numerous green assemblies were observed when the modified chip was incubated with the bio-LPETGG/GGGK-bio/SrtA/FITC-SA mixture (panel d). The above results demonstrated that the ligation product induced the assembly of FITC-SA on the chip surface. Accordingly, SrtA can be determined by examining the *in-situ* generation of $(SA\text{-}bio\text{-}LPETGGGK\text{-}bio)_n$ assemblies.

The analytical performances of the method were investigated by measuring the impedance change in the case of SrtA with various concentrations. As shown in Fig. 3A, the impedance was enhanced with the increase of SrtA concentrations from 0 to 0.1 nmol/L, indicating that the higher level of SrtA could promote the

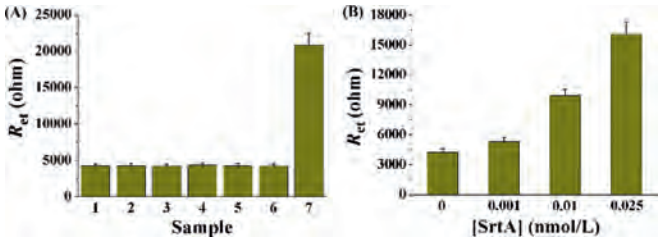

Fig. 4. (A) Selectivity of the method. 1, blank (buffer); 2, ALP; 3, trypsin; 4, lysozyme; 5, thrombin; 6, β-galactosidase; 7, SrtA. The concentration of SrtA was 0.05 nmol/L, and that of other proteins was 5 nmol/L. (B) Dependence of R_{et} on the concentration of SrtA in serum. The concentrations of the spiked SrtA were 0, 0.001, 0.01 and 0.025 nmol/L.

generation of more ligation products. The curve reached to a platform in the presence of high concentrations of SrtA, which might be ascribed to the saturation of the electrode by the SA assemblies. A linear correlation between R_{et} and SrtA concentration was attained in the range of 1–25 pmol/L (Fig. 3B), and the correlation equation could be expressed as $R_{et} = 5076 + 460{,}046$[SrtA] (nmol/L). The relative standard deviations (RSDs) for the detection of various concentrations of SrtA are all less than 10%, indicating an acceptable repeatability of this method. The lowest detectable concentration of 1 pmol/L is much lower than those acquired by HPLC assays (> 100 nmol/L) [36] and fluorescent methods (0.3 nmol/L and 12.5 pmol/L) [11,13], which could be attributed to the high sensitivity of EIS and poor conductivity of protein/peptide assemblies. Moreover, the ligation reaction performed in the homogeneous format and the "one-pot" surface-tethered analysis in the heterogeneous format improved the catalytic efficiency and simplified the detection procedures. The strategy by converting homogeneous reaction to surface-tethered assay may be valuable for designing novel heterogeneous sensing platforms.

To evaluate the specificity of the method, several important enzymes in human body were tested, including alkaline phosphatase (ALP), trypsin, lysozyme, thrombin and β-galactosidase. As shown in Fig. 4A, only SrtA induced a significant increase in the impedance, while all the other enzymes only caused negligible change in the R_{et}. The excellent sensitivity and selectivity allowed for the detection of SrtA in complicated biological samples. As depicted in Fig. 4B, the serum did not lead to significant R_{et}. However, after SrtA was spiked in the serum, the R_{et} was enlarged with increasing concentrations of spiked SrtA. The SrtA concentrations found in the serum were almost coincident with those in the buffer solution. Therefore, the electrochemical method is more suitable for the determination of SrtA in biological samples since serum exhibits significant interference on the AuNPs-based colorimetric assays [37].

SrtA in the Gram-positive pathogenic bacteria plays an important role in human tissue infection. As a typical Gram-positive pathogen, *S. aureus* can cause hospital- and community-acquired infections [28,38]. The feasibility of the method for assay of SrtA in *S. aureus* has been demonstrated. A smaller R_{et} was obtained when the SA-modified electrode was treated by the mixture of SA and *S. aureus* extract, while a higher R_{et} was attained when the extract was pre-incubated with the substrate peptides (bio-LPETGG and GGGK-bio), and then SA. This indicated that SrtA maintained the enzymatic activity in *S. aureus*. As shown in Fig. S3 (Supporting information), the R_{et} was intensified as the concentration of *S. aureus* increased in the range of 1–100 CFU/mL. Berberine chloride can inhibit the activity of SrtA in *S. aureus* [11]. We found that the R_{et} increased much more slowly with the addition of berberine chloride to the extract of *S. aureus* ranging from 1 CFU/mL to 1000 CFU/mL. The proposed method thus holds great potential for determination of SrtA in *S. aureus* bacteria and screening of effective SrtA inhibitor drugs.

In summary, a concept for ligase detection and inhibitor screening by conversion of aggregation-based homogeneous analysis into surface-tethered electrochemical assay has been proposed. SrtA was tested as the model analyte. In the colorimetric assay, the ligation products caused the aggregation of SA-AuNPs, while those in the electrochemical analysis induced the *in-situ* SA assembly. Although the colorimetric assay exhibited poor sensitivity, it possessed the merits of easy operation, fast response time and simple instrumentation, thus providing a viable means for high-throughput screening of potential enzyme inhibitors. Conversely, the electrochemical method showed high sensitivity and selectivity, and involved less sample consumption, holding great promise for the detection of SrtA in complicated biological samples. The feasibility of the electrochemical method for assay of SrtA has been demonstrated both *in vitro* and in *S. aureus*. The lowest detectable concentration of 1 pmol/L is much lower than those by the HPLC assays (> 100 nmol/L) [36] and fluorescent methods (0.3 nmol/L and 12.5 pmol/L) [11,13]. We believe that the assays based on the SA-biotin interactions can be extended to determine other ligases by adopting the sequence-specific substrates.

Declaration of competing interest

The authors declare that they have no known competing financial interests or personal relationships that could have appeared to influence the work reported in this paper.

Acknowledgements

This work was supported by the National Natural Science Foundation of China (Nos. 22076221, 21876208), the Program for Innovative Research Team of Science and Technology in the University of Henan Province (No. 21IRTSTHN005) and the Hunan Provincial Science and Technology Plan Project, China (No. 2019TP1001).

Supplementary materials

Supplementary material associated with this article can be found, in the online version, at doi:10.1016/j.cclet.2021.10.038.

References

[1] R.E. Thompson, T.W. Muir, Chem. Rev. 120 (2020) 3051–3126.
[2] Y. Zhang, K.Y. Park, K.F. Suazo, M.D. Distefano, Chem. Soc. Rev. 47 (2018) 9106–9136.
[3] C. Freund, D. Schwarzer, ChemBioChem 22 (2021) 1347–1356.
[4] Q. Sun, Q. Chen, D. Blackstock, W. Chen, ACS Nano 9 (2015) 8554–8561.
[5] S. Xu, Z. Zhao, J. Zhao, Chin. Chem. Lett. 29 (2018) 1009–1016.
[6] U. Markel, K.D. Essani, V. Besirlioglu, et al., Chem. Soc. Rev. 49 (2020) 233–262.
[7] Y. Zhou, H. Yin, W. Zhao, S. Ai, Coordin. Chem. Rev. 424 (2020) 213519.
[8] T. Cao, J. Lv, L. Zhang, et al., Anal. Chem. 90 (2018) 14303–14308.
[9] F.B.H. Rehm, T.J. Tyler, K. Yap, et al., Angew. Chem. Int. Ed. 59 (2020) 1–6.
[10] S. Eissa, M. Zourob, Analyst 145 (2020) 4606–4614.
[11] Y. Li, Y. Yang, C. Zhang, Anal. Chem. 90 (2018) 13007–13012.
[12] H. Wang, J. Li, Y. Wang, et al., Anal. Chem. 82 (2010) 7684–7690.
[13] J. Zhang, M. Wang, R. Tang, et al., Anal. Chem. 90 (2018) 3245–3252.
[14] G. Chen, Y. Xie, H. Zhang, et al., RSC Adv. 4 (2014) 6560–6563.
[15] X. Ding, D. Ge, K.L. Yang, Sens. Actuat. B 201 (2014) 234–239.
[16] C. Guarise, L. Pasquato, V.D. Filippis, P. Scrimin, Proc. Natl. Acad. Sci. U. S. A. 103 (2006) 3978–3982.
[17] X. Liu, Y. Wang, P. Chen, et al., Anal. Chem. 86 (2014) 2345–2352.
[18] Y. Zhao, L. Cui, W. Ke, et al., ACS Sustain. Chem. Eng. 7 (2019) 5157–5166.
[19] D.Y. Kim, S. Shinde, R. Saratale, et al., Microchim. Acta 184 (2017) 4695–4704.
[20] H. Ravan, A. Norouzi, N. Sanadgol, E. Hosseinzadeh, Microchim. Acta 187 (2020) 392.
[21] T. Wei, T. Dong, Z. Wang, et al., J. Am. Chem. Soc. 137 (2015) 8880–8883.
[22] L. Wu, Y. Wang, X. Xu, et al., Chem. Rev. 121 (2021) 12035–12105.
[23] C. Chen, X. Ji, Chin. Chem. Lett. 29 (2018) 1287–1290.
[24] H. Zhao, E. Su, L. Huang, et al., Chin. Chem. Lett. 33 (2022) 743–746.
[25] F. Xuan, X. Luo, I.M. Hsing, Anal. Chem. 84 (2012) 5216–5220.
[26] Y. Tan, X. Wei, Y. Zhang, et al., Anal. Chem. 87 (2015) 11826–11831.

[27] L. Lu, H. Su, F. Li, Anal. Chem. 89 (2017) 8328–8334.
[28] M.W. Popp, H.L. Ploegh, Angew. Chem. Int. Ed. 50 (2011) 5024–5032.
[29] R. Warden-Rothman, I. Caturegli, V. Popik, A. Tsourkas, Anal. Chem. 85 (2013) 11090–11097.
[30] J.E. Glasgow, M.L. Salit, J.R. Cochran, J. Am. Chem. Soc. 138 (2016) 7496–7499.
[31] Z. Zou, H. Alibiglou, D.M. Mate, et al., Chem. Commun. 54 (2018) 11467–11470.
[32] Y. You, S. Lim, S. Gunasekaran, ACS Appl, Nano Mater. 3 (2020) 1900–1909.
[33] Z. Wang, R. Lévy, D.G. Fernig, M. Brust, J. Am. Chem. Soc. 128 (2004) 2214–2215.
[34] J.R. Waldeisen, T. Wang, B.M. Ross, L.P. Lee, ACS Nano 5 (2011) 5383–5389.
[35] R. D'Agata, P. Palladino, G. Spoto, Beilstein J. NanoTechnol. 8 (2017) 1–11.
[36] R.G. Kruger, P. Dostal, D.G. McCafferty, Anal. Biochem. 326 (2004) 42–48.
[37] C.C. Chang, C.P. Chen, C.-.H. Lee, et al., Chem. Commun. 50 (2014) 14443.
[38] X. Tao, Z. Liao, Y. Zhang, et al., Chin. Chem. Lett. 32 (2021) 791–795.